

## Full paper

## Self-healing: A new skill unlocked for ultrasound transducer

Jiapu Li<sup>a,b,c,h,1</sup>, Yang Yang<sup>d,1</sup>, Zeyu Chen<sup>e</sup>, Shuang Lei<sup>a</sup>, Maokang Shen<sup>a</sup>, Tao Zhang<sup>a</sup>,  
Xuekai Lan<sup>a</sup>, Yijie Qin<sup>a</sup>, Jun Ou-Yang<sup>a</sup>, Xiaofei Yang<sup>a</sup>, Yong Chen<sup>f</sup>, Ziyu Wang<sup>g,\*\*</sup>,  
Benpeng Zhu<sup>a,b,c,h,\*</sup>

<sup>a</sup> School of Optical and Electronic Information, Wuhan National Laboratory for Optoelectronics, Huazhong University of Science and Technology, Wuhan, 430074, China

<sup>b</sup> Engineering Research Center for Functional Ceramics, Ministry of Education, Huazhong University of Science and Technology, Wuhan, 430074, China

<sup>c</sup> Shenzhen Huazhong University of Science and Technology Research Institute, Shenzhen, 518057, China

<sup>d</sup> Department of Mechanical Engineering, San Diego State University, 5500 Campanile Drive, San Diego, CA 92182-1323

<sup>e</sup> College of Mechanical & Electrical Engineering, Central South University, Changsha, 410083, China

<sup>f</sup> Epstein Department of Industrial and Systems Engineering, Department of Aerospace and Mechanical Engineering, Viterbi School of Engineering, University of Southern California, 3715 McClintock Ave, Los Angeles, CA, 90089-01932, USA

<sup>g</sup> The Institute of Technological Sciences, Wuhan University, Wuhan, 430072, China

<sup>h</sup> State Key Laboratory of Transducer Technology, Chinese Academy of Sciences, Shanghai, 200050, China

## ARTICLE INFO

## Keywords:

Self-healing  
Nanocomposite  
Optoacoustic transducer  
Laser-generated ultrasound  
Thrombolysis

## ABSTRACT

For an ultrasound device, to prolong its lifetime and guarantee the performance is of significant importance. Actually, it is difficult for a traditional piezoelectric ultrasound transducer to recover from physical damage caused by sudden impact, accidental scratches, and fatigue fracture. As a promising ultrasound device, the optoacoustic transducer, the core part of which is inorganic-polymer nanocomposite, has drawn much attention in recent years. Fortunately, the development of self-healable polymer provides a good chance for us to endow this kind of device with self-healing capability. Here, based on a covalently cured poly(urea-urethane) elastomeric network and carbon nanotubes nanocomposite, we introduce a catalyst-free and room temperature self-healing optoacoustic transducer. Such device is designed to have a three-layered structure—self-healing nanocomposite/PDMS/glass. By taking the advantage of the principle of wave superposition, its laser-generated ultrasound can be enhanced greatly. This novel ultrasound transducer behaves excellent self-healing performance, and it can recover from a cut or laser-induced damage. After 10th self-repairs, its output can still maintain 92.3% of the original sound pressure. With a self-focusing technology, the developed device can produce high intensity ultrasound (29.2 MPa); after a self-healing process, its laser-generated ultrasound can be kept as high as 28.7 MPa, which is comparable to those values reported in previous literatures with the same laser energy input. Most importantly, such high intensity ultrasound can be successfully used for thrombolysis. These promising results demonstrate that the obtained self-healing ultrasound device is suitable for biomedical applications, which may open a new path for smart biomedical device design and fabrication in the future.

## 1. Introduction

Scientific inspiration usually comes from natural system [1]. Recently, inspired by the wound healing properties of the skin, to endow functional device with self-healing capability has fascinated many scientists. Since incidental scratches or mechanical cuts may destroy device's performance, only the self-healable one can benefit from

long-term use as well as enhanced reliability, maintenance and durability [2]. Reportedly, much effort has been being carried out to investigate self-healable devices, such as wearable sensor [3], supercapacitor [4], electrochemical device [5], and solar cell [6]. Little attention, however, is being paid to self-healable ultrasound transducer.

Ultrasound transducer is widely used for biomedical imaging [7], clinical therapy [8], neuro stimulation [9], and cell manipulation [10],

\* Corresponding author. School of Optical and Electronic Information, Wuhan National Laboratory for Optoelectronics, Huazhong University of Science and Technology, Wuhan, 430074, China.

\*\* Corresponding author.

E-mail addresses: [zywang@whu.edu.cn](mailto:zywang@whu.edu.cn) (Z. Wang), [benpengzhu@hust.edu.cn](mailto:benpengzhu@hust.edu.cn) (B. Zhu).

<sup>1</sup> Jiapu Li and Yang Yang contribute equally to this paper.

11], so to prolong its lifetime and guarantee the performance is of significant importance. Nevertheless, traditional ultrasound transducer is based on piezoelectric materials, and does possess no self-healing capability. Optoacoustic transducer, a promising candidate in ultrasound device family, has drawn much attention in recent years owing to its high power density and broad bandwidth [12–14]. Unlike the piezoelectric ultrasound device, the principle of optoacoustic transducer is photoacoustic effect and its core part is inorganic-polymer nanocomposite. When the nanocomposite is irradiated by a pulsed-laser, local heating occurs, and periodic thermal expansion happens, resulting in the generation of acoustic wave. To the best of our knowledge, most of the self-healable structures usually depend on polymeric materials [4,15–17]. There are several methods for creating self-healing polymeric materials: the storage of healing agents (hollow fibers, microcapsules), reversible covalent bond formation with external stimuli (Diels-Alder, or DA, reaction, disulfide groups, and thiols), and the construction of healing materials by non-covalent bonds [18–25]. Its development provides us with an efficient way to design the nanocomposite based self-healable optoacoustic transducer.

Here, we introduce poly(urea-urethane) elastomer, a catalyst-free and room temperature self-healing material, to the ultrasound transducer fabrication process. The influence of CNTs concentration in this nanocomposite on its acoustic performance and self-healing behavior was investigated, and the optimal value was determined. A special three-layered device configuration was studied theoretically and experimentally, and the output ultrasound was greatly improved. To demonstrate its excellent self-healing property, both cut and laser-induced damage were introduced to the developed device. To further prove the feasibility of biomedical application, a thrombolysis experiment was successfully conducted using a focused self-healing optoacoustic transducer.

## 2. Experimental section

### 2.1. Fabrication of self-healing optoacoustic transducer

The self-healing polymer was prepared according to the reference [26]. Due to its excellent absorbance and thermal conduction [13], CNTs with a diameter of 8 nm and a length of 10–30  $\mu\text{m}$  was selected. Then, the CNTs (0.2 g) were dispersed into self-healing polymer (2 g) by magnetic stirring for 10 min, followed by thermal cross-linking with urea. The interaction between CNTs and poly(urea-urethane) elastomeric by hydrogen bonds can hold the shape of poly(urea-urethane) elastomeric networks. The mixture (self-healing polymer/CNTs) was degassed under vacuum for 15 min. For Type I transducer fabrication, the composite was deposited directly on glass substrate using spinning technology (1000 rpm for 30 s), then it was cured at 60 for 16 h. For Type II transducer fabrication, the PDMS was spun on the glass substrate with the speed of 2000 rpm for 30 s. After PDMS layer was degassed (under vacuum for 15 min) and cured (110  $^{\circ}\text{C}$  for 5 min), the self-healing composite with the same thickness as Type I was deposited on it.

### 2.2. Characterization and testing

The morphologies were characterized by the field-emission gun scanning electron microscope (Sirion 200 from FEI) and transmission electron microscopy (Tecnai G2 F30 from FEI). Mechanical tensile-stress experiments were performed by using the electronic dynamic static universal material testing machine (ElectroPuls E10000 from Instron). Tensile experiments were carried out at room temperature (25  $^{\circ}\text{C}$ ) at a strain rate of 5 mm  $\text{min}^{-1}$ . Healing experiments were conducted at room temperature just by putting damaged pieces together. The semiconductor device analyzer (B1500A from Agilent) was utilized to measure samples' resistance variation. The absorbance of the optoacoustic transducer was tested by ultraviolet and visible spectrophotometer (Lambda 35, PerkinElmer, USA). In the laser-generated ultrasound experiment, a 6 ns pulsed laser ( $\lambda = 532 \text{ nm}$ ) with a repetition rate of 20

Hz (Lapa-80 from Lei Bao Optoelectronics Technology Co., Ltd) was employed. The laser beam, whose initial aperture size is 5 mm, penetrated through a transparent wall of the water tank and shined on the self-healing optoacoustic transducer. A piezoelectric hydrophone with 0.2 mm diameter (Precision Acoustic, UK) was used to detect the acoustic wave, which was recorded by an oscilloscope (TDS-2024B, Tektronix, USA).

## 3. Results and discussion

Fig. 1A shows the manufacturing process of the poly(urea-urethane) and CNTs nanocomposite. Based on the metathesis reaction of the aromatic disulfides, the poly(urea-urethane) elastomer, after being cut in half with a razor blade, can self-mend by simple contact at room temperature without the need of any catalyst or stimulation [26]. The self-healing mechanism is illustrated in Supplementary Fig. S1. To visualize the self-healing performance of the poly(urea-urethane) and CNTs nanocomposite, as shown in Fig. 2B, a commercial available light-emitting diode (LED) bulb was employed. When the composite switches from damaged to full recovery, the LED changes from extinguished to gradually lighted up. Fig. 1C (time cycles) describes the change of electrical resistance with the healing cycles. Obviously, the electrical conductivity is determined by the proximity of the CNTs in nanocomposite. Its high electrical healing efficiency originates from the re-association of the hydrogen bonds within the polymer that allows CNTs to be closely packed at the healing interface. Most importantly, its electrical conductivity can recover from the repeated cuts, demonstrating the outstanding self-healing capability of this nanocomposite. Fig. 1D shows the variation of the stress-strain curves with the healing time for the self-healing nanocomposite. Taking into account the restoration of both stress and strain (area under the stress-strain curve), mechanical healing efficiency can be quantified using toughness [27]. For the calculation of mechanical healing efficiency, please refer to the supporting information (1). At room temperature, when the self-healing time was 0.5 h, 1 h, and 12 h, the maximum tensile stress was restored to 63.1%, 77.3%, and 96.6%, meanwhile, the mechanical healing efficiencies reached 37.9%, 51.8%, and 87.6%, respectively.

Fig. 2A illustrates the structure design for two types of optoacoustic transducers. For both types of transducer, the CNTs concentration in self-healing nanocomposite is the same and the only difference is the PDMS layer. To determine the optimum value of CNTs concentration, four groups of samples with 5 wt%, 6.7 wt%, 10 wt%, and 14.3 wt% CNTs were prepared. As depicted in Fig. 2B, for the light with the wavelength of 532 nm, the absorbance of the optoacoustic transducer obviously increases with CNTs concentration increasing; and the absorbance reaches saturation when the CNTs concentration is higher than 10 wt%. Additionally, the CNTs concentration also affects the device's self-healing performance (Fig. S2, Supporting Information). In the inset of Fig. 2B, it is easy to see that the composite with 10 wt% CNTs is healable, but the sample with 14.3 wt% CNTs lost the self-healing capability. The reason may be probably that surface area of the fractured interface is mainly occupied by CNTs, which prevents the polymer from contacting each other. To seek to a compromise between absorption and self-healing performance, the composite with 10 wt% CNTs was selected for optoacoustic transducer fabrication. As shown in Fig. 2C, for each optoacoustic transducer, the peak pressure is in direct proportional to the laser energy; for the same device structure, the higher the CNTs concentration is, the better the acoustic performance will be. It is worth noting that, compared with Type I transducer, Type II transducer exhibits a superior acoustic behavior under the same laser energy density. It suggests that the function of PDMS layer is to enhance the ultrasound generation, as depicted in Fig. 2D and E. In the inset, the cross-section SEM images of the self-healing optoacoustic transducer are illustrated, and the thicknesses of the self-healing composites and PDMS layer are  $\sim 200 \mu\text{m}$  and  $\sim 35 \mu\text{m}$ , respectively. The optoacoustic conversion efficiency of Type II transducer can be calculated using the following

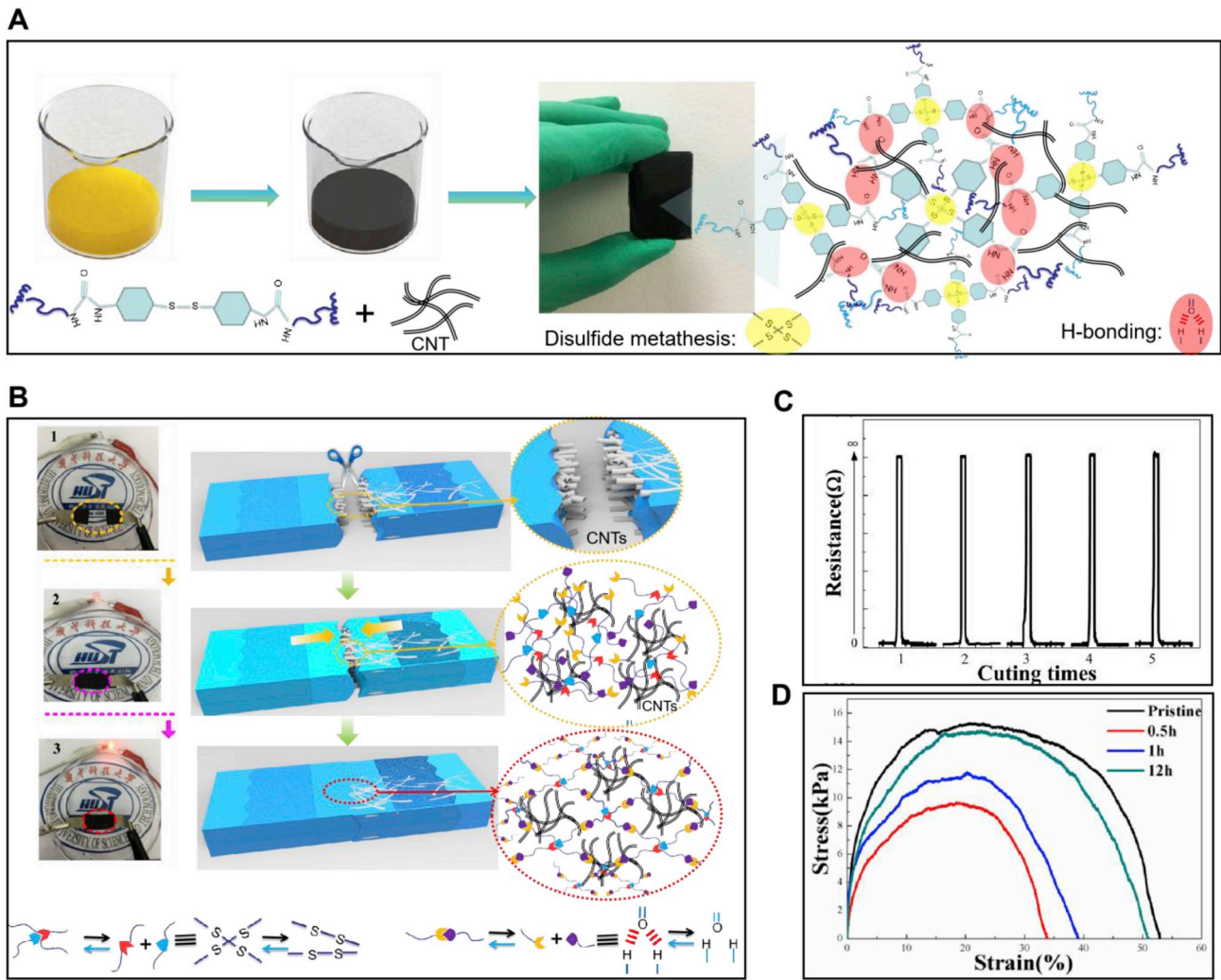


**Fig. 1.** (A) The preparation process of the self-healing materials. (B) The self-healing of electrical conductivity and schematic representation of self-healing capabilities of the poly(urea-urethane) and CNT composite. (C) Repeated electrical healing for five cuts at the same severed location. (D) Strain-stress curves of original and healed sample for different healing time.

equation:

$$\eta = \frac{E_a}{E_{\text{optical}}} \quad (1)$$

$$E_a = \frac{1}{\rho C} A \int P^2(t) dt \quad (2)$$

where  $P(t)$ ,  $A$ ,  $\rho$ ,  $C$ ,  $E_{\text{optical}}$  and  $E_a$  are the acoustic pressure, the laser area, the water's density, ultrasound speed in water, pulse laser's energy and the energy of the acoustic signal, respectively. The value of  $\eta$  can be determined to be approximately  $2.93 \times 10^{-3}$ , which is in the range of our previous results for CNT-PDMS composite transducers ( $1.32\text{--}9.59 \times 10^{-3}$ ) [13].

Evidently, due to a superior thermal expansion coefficient [29], the PDMS layer can indeed improve the system's thermal expanding, which is beneficial for the ultrasound output. Furthermore, as laser absorption and thermal transmission are limited in range of just several micrometers along  $x$  axis, it can be supposed that the ultrasound is generated at the interface of PDMS and self-healing nanocomposite, as presented in Fig. 3A. The laser-generated ultrasound can propagate forward (F wave) and backward (B wave), simultaneously. Actually, the glass's acoustic impedance is much larger than that of PDMS, so B wave is thought to be reflected by the glass substrate and has the same polarity after the reflection [30]. Since ultrasound's velocity in PDMS is 1480 m/s and the

PDMS layer's thickness is in the order of tens of micrometers in our design, the delayed time between F wave and B wave is  $\sim$ ns. Therefore, the measured ultrasound signal probably is the result of two acoustic waves' superposition, as shown in Fig. 3B. Consequently, the thickness of the PDMS layer determines the delayed time and is so crucial.

According to our previous work [28,29], F wave's acoustic pressure and B wave's acoustic pressure in the water can be expressed as  $P_1$  and  $P_2$ , respectively. (Supporting Information (2))

$$P_1(x, t) = D_1 e^{j\omega t - k_1(x-h)} \quad (3)$$

$$P_2(x, t) = D_1 e^{j\omega(t+(h+2l)/c) - k_1(x-h)} \quad (4)$$

Taking into account two waves' superposition [30,31], the theoretical acoustic pressure for Type II transducer can be represented below:

$$P(x, t) = D_1 (e^{j\omega t - k_1(x-h)} + e^{j\omega(t+(h+2l)/c) - k_1(x-h)}) \quad (5)$$

In equation (5),  $l$  is the thickness of PDMS layer. As shown in Fig. 3C and D, we change the value of thickness, and different waveform can be obtained theoretically and experimentally. It can be found that the measured results are in good agreement with the simulated ones. For Type I transducer, no PDMS exists, so  $l = 0$ . For Type II transducer, the optimum thickness of PDMS layer is approximately 35  $\mu\text{m}$ , where F wave and B wave can overlap to form a single echo.



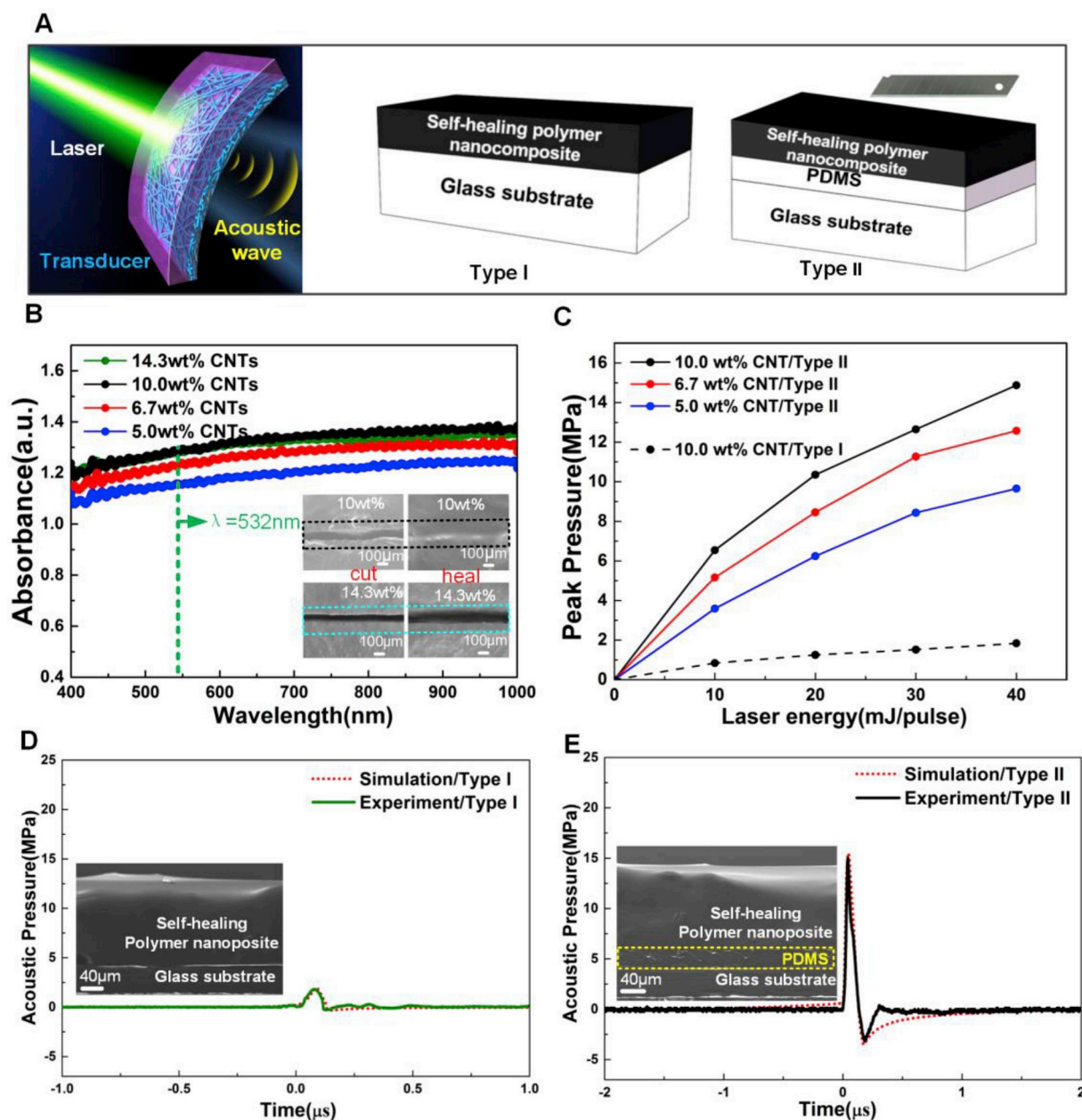


**Fig. 2.** (A) Schematic diagram of self-healing optoacoustic transducer: Type I (self-healing composite/glass substrate) and Type II (self-healing composite/PDMS/glass substrate). (B) Absorbance of optoacoustic transducers with the different CNT concentration. (C) Peak pressure produced by optoacoustic transducer with the different CNT concentration under different energy density. Comparison of simulation and experiment results of laser-generated ultrasound signal for Type I (D) and Type II (E) optoacoustic transducers.

For an optoacoustic transducer, sound pressure is a crucial parameter, which can be used to evaluate the self-healing performance. As illustrated in Fig. 4A, Type II transducer can produce ultrasound around 15 MPa when the laser energy is 40 mJ/pulse. Once it undergoes a cut damage, the acoustic pressure is reduced to 9 MPa. Fortunately, after 12 h self-healing process, this device can be restored almost to its initial state. COMSOL Multi-physics simulation results of the acoustic pressure before and after cutting agree well with the measured ones (Fig. 4B and C). As shown in Fig. 4D, the peak pressure of Type II transducer slightly decreases with the increased healing cycles. Meanwhile, the operational frequency remains nearly invariable ( $\sim 2.5$  MHz). After 1st and the 10th repairs, the value of peak pressure can still reach 98.3% and 92.3% of the original one, respectively. The slight decrease is probably related to self-healing polymer. The more the healing cycle is, the longer time for the restoration interface to contact with surrounding environment will

be. The absorption of moisture may cause a loss of hydrogen-bonding ability.

Practically, the physical damage may be caused by the laser itself if its energy is too high. Fig. 5A shows the schematic diagram of the self-healing process of the developed transducer from laser damage at room temperature. After being irradiated by a laser with the power of 50 mJ/pulse for 5 mins, a wound with a diameter of approximately 500  $\mu$ m appears in the poly(urea-urethane) and CNTs nanocomposite (Fig. 5B and C). The wounded device can recover itself after 12 h healing time, and its acoustic pressure can reach around 94.1% of the initial value before damage (Fig. 5D). Obviously, the laser damage is bigger than that of a cut. It is reasonable that the former's acoustic pressure recovery coefficient (94.1%) is slightly lower than that (98.3%) of the latter one. In Fig. 5E–G, the acoustic pressure simulations are in good accordance with the experimental ones. This result demonstrates the reliability of

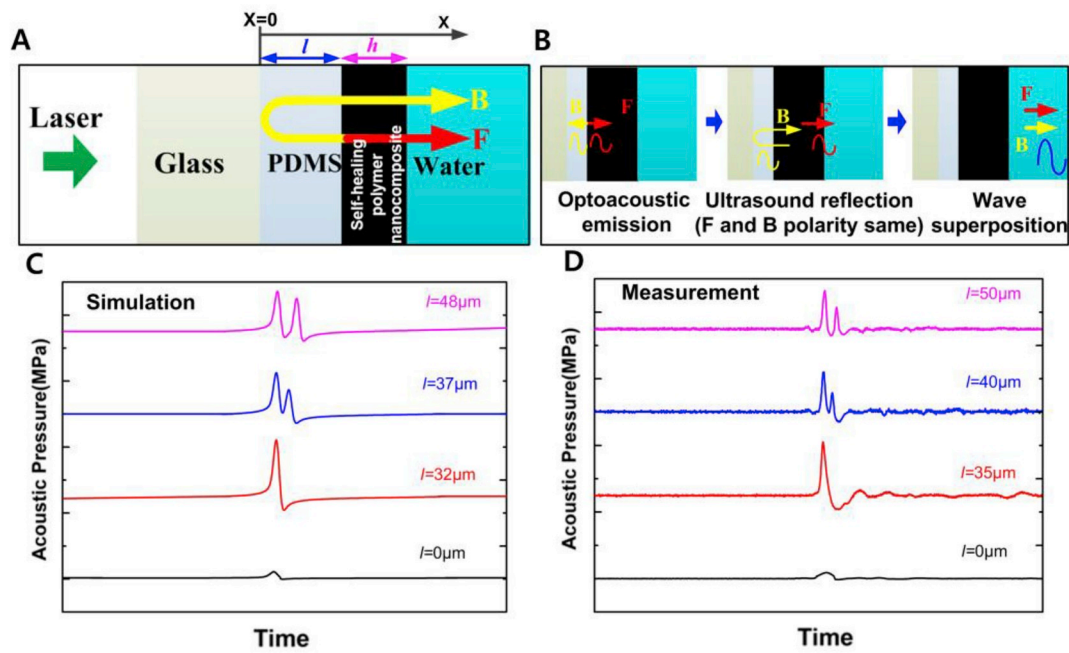


Fig. 3. (A) Schematic diagram of laser-generated ultrasound signal propagation process; F: forward wave; B: backward wave. (B) Schematic diagram of ultrasound wave superposition process, including ultrasound emission, reflection and interference. Theoretical (C) and experimental (D) analysis of the effect of PDMS layer's thickness on acoustic performance.

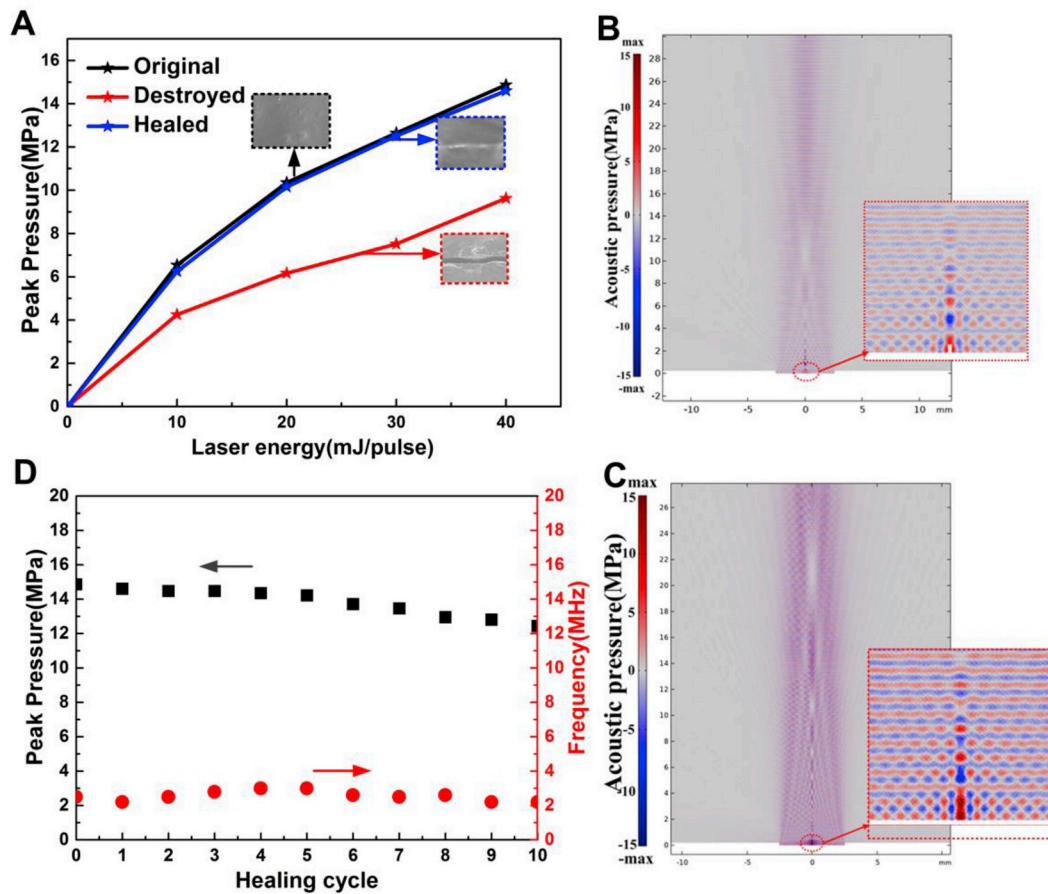
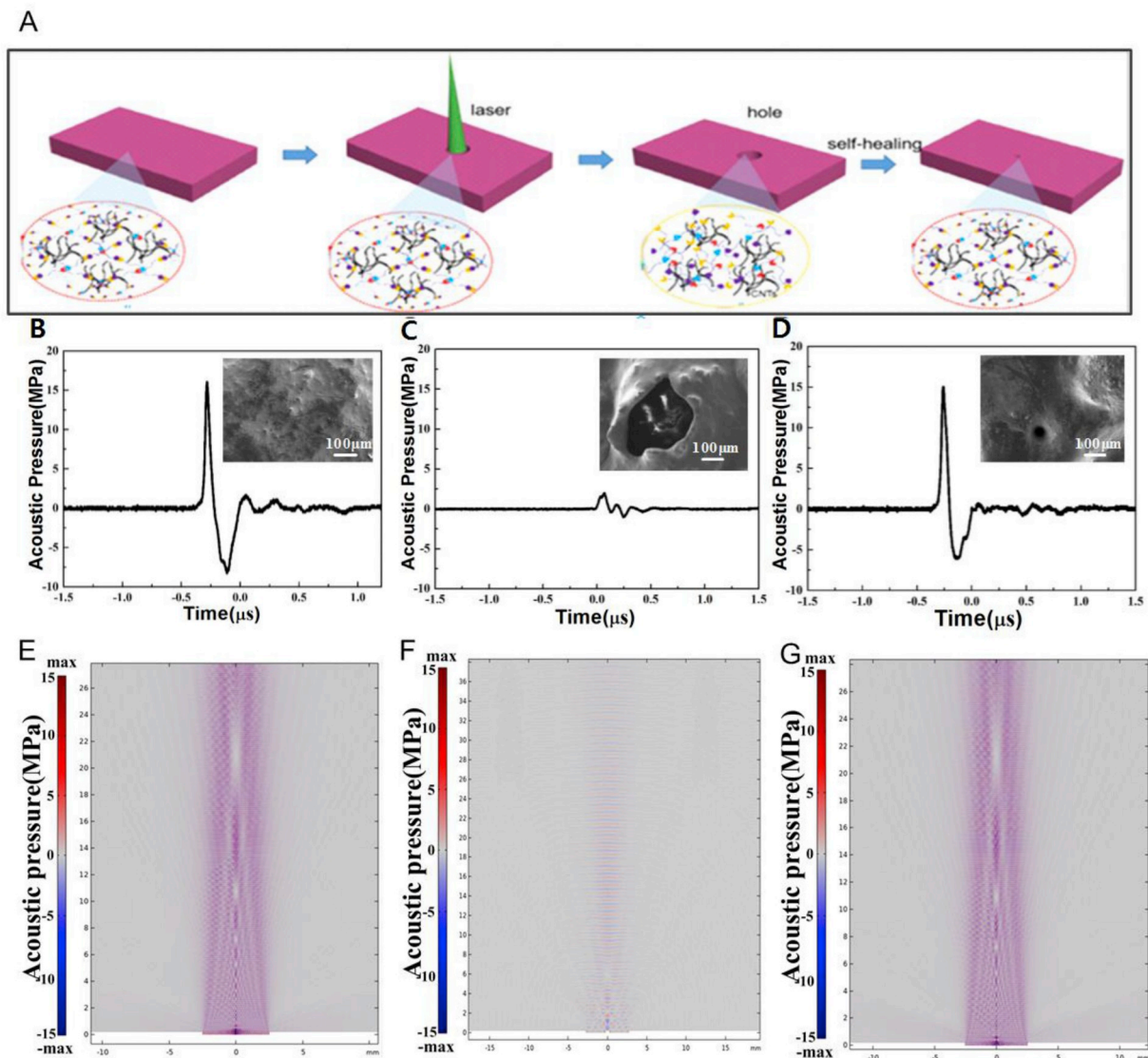


Fig. 4. (A) Comparison of laser-generated ultrasound signals for Type II transducer in initial state (black line), when damaged (blue line) and after self-healing (red line). Simulations of acoustic pressure for the Type II transducer when damaged (B) and after self-healing (C). (D) The variation of scoustic signal characteristics of Type II transducer with the healing cycle.



**Fig. 5.** (A) Schematic diagram of optoacoustic self-healing transducer damaged by a high energy laser and its self-healing process at room temperature. Acoustic pressure and SEM images of the optoacoustic device at original state (B), damaged by laser (C) and after self-healing (D). Acoustic pressure simulation of the optoacoustic device at the original state (E), damaged by laser (F) and after self-healing (G).

this optoacoustic device again.

High intensity focused ultrasound plays an important role in clinical therapy [32,33]. To meet the requirement of such high power application, a focused ultrasound transducer is needed. Traditional piezoelectric transducer easily becomes broken during this application process and can't be used again. To overcome this issue, we fabricate a self-healing optoacoustic transducer using a self-focusing technology. A self-focused glass substrate is employed to replace that planar one in Type II transducer. In our design, focal distance is  $r = 9$  mm, and the aperture is  $D = 15$  mm, so f-number of this ultrasound device is 0.6. As shown in Fig. 6A, when the laser energy is 20mJ/pulse, the output acoustic pressure at the focal point is measured to be 29.2 MPa. Most importantly, after a self-recovery process from a cut damage, the focused optoacoustic transducer can produce ultrasound as high as 28.7 MPa. As shown in Table 1, it is noticed that these two values are comparable to those focused acoustic pressure reported by Jiang's group (~27 MPa) [34] and Guo's group (~33 MPa) [35] with the same laser energy input. If we continue to increase the laser energy to 40mJ/pulse, its acoustic pressure is estimated to be ~50 MPa, unfortunately, which is beyond the measurement range of hydrophone ( $\leq 30$  MPa).

To the visualize the high intensity focused ultrasound, a Tofu sample

treatment experiment is carried out (supporting video 1). Fig. 6B shows the photographs of Tofu sample before and after the treatment. Apparently, the focused laser-generated ultrasound is strong enough and can drill a hole in Tofu sample. To demonstrate the possibility of practical application for this developed device, a thrombolysis experiment is conducted. The animal blood clot, as depicted in Fig. 6C, is selected and put inside a pipe at the focal point of the ultrasound transducer. This transducer is the one that undergoes a self-healing process from a cut damage. Evidently, when high intensity focused ultrasound is applied to the blood clot, its volume begins to decrease, indicating that blood clot can be dissolved. Its mechanism for sonothrombolysis could be either stable cavitation or inertial cavitation [33]. This process is recorded by a video (supporting video 2). It is clear to observe that, after high intensity focused ultrasound treatment, the blood clot becomes smaller, as shown in Fig. 6D. These promising results suggest that this developed self-healing optoacoustic transducer is suitable for potential application in biomedical technology.

Supplementary video related to this article can be found at <https://doi.org/10.1016/j.nanoen.2019.104348>.



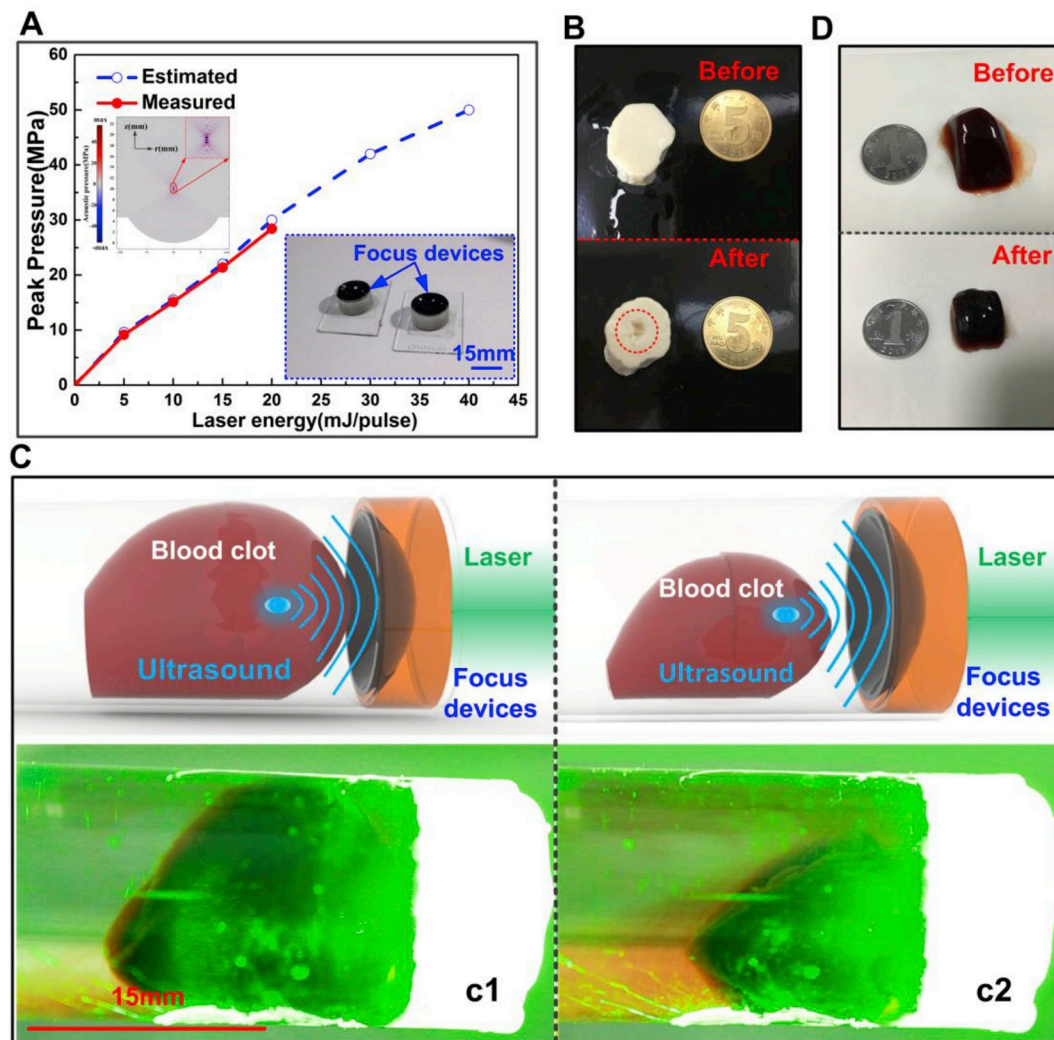


**Fig. 6.** (A) The measured and simulated focused acoustic pressure; Inset: the photograph of focused device. (B) Tofu sample before and after focused high intensity ultrasound treatment. (C) Schematic diagram and photograph for thrombolytic experiment. (D) Blood clot before and after focused high intensity ultrasound treatment.

**Table 1**  
Acoustic pressure and experimental parameters comparison.

References	Optically absorbing Material	Laser energy (mJ/pulse)	Backing substrate	Acoustic pressure (MPa)
[13]	CNTs	35	Planar	24.4
[34]	Carbon black	18	Focused	22.5
[35]	CNTs	20	Focused	~33
This work	CNTs	40	Planar	15
This work	CNTs	20	Focused	29.2

#### 4. Conclusion

In summary, we have successfully fabricated a catalyst-free room temperature self-healable optoacoustic transducer with a special three-layered structure—self-healing nanocomposite/PDMS/glass. Such device's self-healing performance is based on a covalently cured poly (urea-urethane) elastomeric network and CNTs nanocomposite, and it can recover from a cut or a laser-induced damage. Even undergoing 10 times self-repair from a damage, the output ultrasound can still maintain 92.3% of the original sound pressure. With a self-focusing technology, a focused self-healing transducer is obtained and its output acoustic pressure at the focal point is measured to be 29.2 MPa when the laser

energy is 20mJ/pulse. It is worthy noticing that its laser-generated ultrasound after a self-recovery process is as high as 28.7 MPa, which is comparable to those focused acoustic pressure reported in literatures with the same laser energy input. Most importantly, using this kind of focused self-healing device, the achievement of thrombolysis has been realized. These promising results demonstrate that this developed self-healing optoacoustic transducer is competent for biomedical applications, which may provide new ideas for design and fabrication of next-generation smart biomedical device.

#### Declaration of competing interest

The authors declare that they have no known competing financial interests or personal relationships that could have appeared to influence the work reported in this paper.

#### Acknowledgments

This work was supported by the Natural Science Foundation of China (Grant no. 11774117), the Natural Science Foundation Instrument Project of China (Grant no. 81727805), Excellent Youth Foundation of Hubei Province (2018CFA083), and the Science and Technology Project of Shenzhen (JCYJ20180305180900394). We also thank the Analytical

and Testing Center of Huazhong University of Science & Technology.

## Appendix A. Supplementary data

Supplementary data to this article can be found online at <https://doi.org/10.1016/j.nanoen.2019.104348>.

## References

- [1] E.D. Elia, S. Barg, N. Ni, V.G. Rocha, E. Saiz, Self-healing graphene-based composites with sensing capabilities, *Adv. Mater.* 27 (2015) 4788–4794.
- [2] T.P. Huynh, P. Sonar, H. Haick, Advanced materials for use in soft self-healing devices, *Adv. Mater.* 29 (2017) 1604973.
- [3] T.F. Wu, B.Q. Chen, A mechanically and electrically self-healing graphite composite dough for stencil-printable stretchable conductors, *J. Mater. Chem. C* 4 (2016) 4150–4154.
- [4] H. Wang, B.W. Zhu, W.C. Jiang, Y. Yang, W.R. Leow, H. Wang, X.D. Chen, A mechanically and electrically self-healing supercapacitor, *Adv. Mater.* 26 (2014) 3638–3643.
- [5] A.J. Bhandarkar, V. Mohan, C.S. López, J. Ramírez, J. Wang, Self-healing inks for autonomous repair of printable electrochemical devices, *Adv. Electron. Mater.* 1 (2015) 1500289.
- [6] S. Banerjee, R. Tripathy, D. Cozzens, T. Nagy, S. Keki, M. Zsuga, R. Faust, Photoinduced smart, self-healing polymer sealant for photovoltaics, *ACS Appl. Mater. Interfaces* 7 (2015) 2064.
- [7] L.V. Wang, J.J. Yao, A practical guide to photoacoustic tomography in the life sciences, *Nat. Mater.* 13 (2016) 627–638.
- [8] L. Lan, Y. Xia, R. Li, K.M. Liu, J.Y. Mai, J.A. Medley, S.O. Gyasi, L.K. Han, P. Wang, J.X. Cheng, A fiber optoacoustic guide with augmented reality for precision breast-conserving surgery, *Light Sci. Appl.* 7 (2018) 2047.
- [9] G. Leinenga, C. Langton, R. Nisbet, J. Götz, Ultrasound treatment of neurological diseases—current and emerging applications, *Nat. Rev. Neurol.* 12 (2016) 161–174.
- [10] B.P. Zhu, C.L. Fei, C. Wang, Y.H. Zhu, X.F. Yang, H.R. Zheng, Q.F. Zhou, K. K. Shung, Self-focused AlScN film ultrasound transducer for individual cell manipulation, *ACS Sens.* 2 (2017) 172–177.
- [11] C.L. Fei, X.L. Liu, B.P. Zhu, D. Li, X.F. Yang, Y.T. Yang, Q.F. Zhou, AlN piezoelectric thin films for energy harvesting and acoustic devices, *Nano Energy* 51 (2018) 146–161.
- [12] H.W. Baac, J.G. Ok, T. Lee, L.J. Guo, Nano-structural characteristics of carbon nanotube-polymer composite films for high-amplitude optoacoustic generation, *Nanoscale* 7 (2015) 14460–14468.
- [13] J.P. Li, X.K. Lan, S. Lei, J. Ou-Yang, X.F. Yang, B.P. Zhu, Effects of carbon nanotube thermal conductivity on optoacoustic transducer performance, *Carbon* 145 (2019) 112–118.
- [14] S. Noimark, R.J. Colchester, B.J. Blackburn, E.Z. Zhang, E.J. Alles, S. Ourselin, P. C. Beard, I. Papakonstantinou, I.P. Parkin, A.E. Desjardins, Carbon-nanotube-PDMS composite coatings on optical fibers for all-optical ultrasound imaging, *Adv. Funct. Mater.* 26 (2016) 8390–8396.
- [15] M.D. Hager, P. Greil, C. Leyens, S.V. Zwaag, U.S. Schubert, Self-healing materials, *Adv. Mater.* 22 (2010) 5424–5430.
- [16] T. Kakuta, Y. Takashima, M. Nakahata, M. Otsubo, H. Yamaguchi, A. Harada, Preorganized hydrogel: self-healing properties of supramolecular hydrogels formed by polymerization of host-guest-monomers that contain cyclodextrins and hydrophobic guest groups, *Adv. Mater.* 25 (2013) 2849–2853.
- [17] T.S. Wong, S.H. Kang, S.K.Y. Tang, E.J. Smythe, B.D. Hatton, A. Grinthal, J. Aizenberg, Bioinspired self-repairing slippery surfaces with pressure-stable omniphobicity, *Nature* 477 (2011) 443–447.
- [18] X. Chen, M.A. Dam, A. Ono, A. Mal, H. Shen, S.R. Nutt, K. Sheran, F. Wudl, Thermally Re-mendable cross-linked polymeric material, *Science* 295 (2002) 1698–1702.
- [19] P. Cordier, F. Tournilhac, C.S. Ziakovic, L. Leibler, Self-healing and thermoreversible rubber from supramolecular assembly, *Nature* 451 (2008) 977–980.
- [20] M. Zhang, D. Xu, X. Yan, J. Chen, S. Dong, B. Zheng, F. Huang, Self-healing supramolecular gels formed by crown ether based host-guest interactions, *Angew. Chem. Int. Ed.* 51 (2012) 7011–7015.
- [21] S. Benight, C. Wang, J.B.H. Tok, Z. Bao, Stretchable and self-healing polymers and devices for electronic skin, *Prog. Polym. Sci.* 38 (2013) 1961–1977.
- [22] S. Bode, L. Zedler, F.H. Schacher, B. Dietzek, M. Schmitt, J. Popp, M.D. Hager, U. S. Schubert, Self-healing polymer coatings based on crosslinked metallo supramolecular copolymers, *Adv. Mater.* 25 (2013) 1634–1638.
- [23] K.S. Toohey, N.R. Sottos, J.A. Lewis, J.S. Moore, S.R. White, Self-healing materials with microvascular networks, *Nat. Mater.* 6 (2007) 581–585.
- [24] J.H. Kang, D.H. Son, G.J.N. Wang, Y.X. Liu, J. Lopez, Y. Kim, J.Y. Oh, T. Katsumata, J. Mun, Y. Lee, L.H. Jin, J.B.H. Tok, Z.N. Bao, Tough and water-insensitive self-healing elastomer for robust electronic skin, *Adv. Mater.* 30 (2017) 1706846.
- [25] Y. Yang, B.P. Zhu, D. Yin, J.H. Wei, Z.Y. Wang, R. Xiong, J. Shi, Z.Y. Liu, Q.Q. Lei, Flexible self-healing nanocomposites for recoverable motion sensor, *Nano Energy* 17 (2015) 1–9.
- [26] A. Rekondo, R. Martin, A.R. Luzuriaga, G. Cabañero, H.J. Grande, I. Odriozola, Catalyst-free room-temperature self-healing elastomers based on aromatic disulfide metathesis, *Mater. Horiz.* 1 (2014) 237–240.
- [27] B.C.K. Tee, C. Wang, R. Allen, Z.N. Bao, An electrically and mechanically self-healing composite with pressure and flexion-sensitive properties for electronic skin applications, *Nat. Nanotechnol.* 7 (2012) 825–832.
- [28] B.Y. Hsieh, J. Kim, J. Zhu, S. Li, X. Zhang, X. Jiang, A laser ultrasound transducer using carbon nanofibers-polydimethylsiloxane composite thin film, *Appl. Phys. Lett.* 106 (2015), 021902.
- [29] Z.Y. Chen, Y. Wu, Y. Yang, J.P. Li, B.S. Xie, X.J. Li, S. Lei, J. Ou-Yang, X.F. Yang, Q. F. Zhou, B.P. Zhu, Multilayered carbon nanotube yarn based optoacoustic transducer with high energy conversion efficiency for ultrasound application, *Nano Energy* 46 (2018) 314–321.
- [30] T. Lee, Q. Li, L.J. Guo, Out-coupling of longitudinal photoacoustic pulses by mitigating the phase cancellation, *Sci. Rep.* 6 (2016) 21511.
- [31] G.J. Diebold, T. Sun, M.I. Khan, Photoacoustic monopole radiation in one, two, and three dimensions, *Phys. Rev. Lett.* 67 (1991) 3384.
- [32] C. Wright, K. Hynynen, D. Goertz, In vitro and in vivo high intensity focused ultrasound thrombolysis, *Investig. Radiol.* 4 (2012) 217–225.
- [33] J.M. Shen, A.D. Liu, Y. Tu, G.S. Foo, C.B. Yeo, M.B. Chan-Park, R.R. Jiang, Y. Chen, How carboxylic groups improve the performance of single-walled carbon nanotube electrochemical capacitors, *Energy Environ. Sci.* 4 (2011) 4220–4229.
- [34] Di Jin, J.W. Kim, Q.Y. Hu, X.N. Jiang, Zhen Gu, Spatiotemporal drug delivery using laser-generated-focused ultrasound system, *J. Control. Release* 220 (2015) 592–599.
- [35] W.B. Hyoun, G.O. Jong, A. Maxwell, K.T. Lee, Y.C. Chen, A.J. Hart, Zhen Xu, E. Yoon, L.J. Guo, Carbon-nanotube optoacoustic lens for focused ultrasound generation and high-precision targeted therapy, *Sci. Rep.* 2 (2012) 1–8.